General Disclaimer

One or more of the Following Statements may affect this Document

- This document has been reproduced from the best copy furnished by the organizational source. It is being released in the interest of making available as much information as possible.

- This document may contain data, which exceeds the sheet parameters. It was furnished in this condition by the organizational source and is the best copy available.

- This document may contain tone-on-tone or color graphs, charts and/or pictures, which have been reproduced in black and white.

- This document is paginated as submitted by the original source.

- Portions of this document are not fully legible due to the historical nature of some of the material. However, it is the best reproduction available from the original submission.

NASA TM X-73460

EFFECT OF EXTERNAL JET-FLOW DEFLECTOR GEOMETRY ON OTW AERO-ACOUSTIC CHARACTERISTICS

by U. von Glahn and D. Groesbeck
Lewis Research Center
Cleveland, Ohio 44135
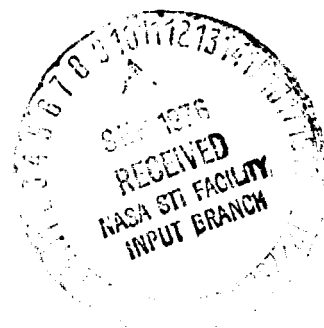
EFFECT OF EXTERNAL JET-FLOW DEFLECTOR GEOMETRY

ON OTW AERO-ACOUSTIC CHARACTERISTICS

by U. von Glahn[1] and D. Groesbeck[2]

V/STOL and Noise Division
Lewis Research Center
Cleveland, Ohio 44135

E-8823

ABSTRACT

The effect of geometry variations in the design of external deflectors for use with OTW configurations was studied at model scale and subsonic jet velocities. Included in the variations were deflector size and angle as well as wing size and flap setting. A conical nozzle (5.2-cm diameter) mounted at 0.1 chord above and downstream of the wing leading edges was used. The data indicate that external deflectors provide satisfactory take-off and approach aerodynamic performance and acoustic characteristics for OTW configurations. These characteristics together with expected good cruise aerodynamics, since external deflectors are storable, may provide optimum OTW design configurations.

INTRODUCTION

The attachment of flow from the exhaust nozzle of an engine-over-the-wing configuration to the wing and flap surfaces can be accomplished by either of two general nozzle design classes. The first nozzle-design class consists of a nozzle which is mounted flush to the wing surface (fig. 1(a)). Attachment of the jet flow to the flap surface is accomplished by angling the top surface of the nozzle toward the wing surface (kickdown

---

[1]Member AIAA; Chief, Jet Acoustics Branch
[2]Aerospace Research Engineer

or roof angle). The upper surface of the nozzle then constitutes an "internal deflector" for the jet flow. Aerodynamic and acoustic data for this type nozzle/wing configuration are discussed, among others, in references 1 to 5. The second nozzle-design class consists of nozzles to which external deflectors are attached to vector the exhaust flow toward the wing surface (fig. 1(b) and (c)). Aero-acoustic data for a limited number of such nozzle/wing configurations are given, among others, in references 1, 2, 6, and 7.

A comparison of the experimental data from references 1 to 7 shows that, in general, the acoustic signitures are similar for STOL-OTW configurations using slot-type nozzles in which the nozzle is located on the wing surface and those using external deflectors to attach the flow to the wing. The acoustic differences that do exist appear to be related to specific design and flow variables peculiar to each nozzle/wing configuration. Thus, the criteria for selecting an optimum nozzle for a STOL-OTW configuration may be determined by considerations other than the configuration acoustics. These criteria may include installed weight, accessibility, design complexity and cruise performance. For example, it can be postulated that for the cruise mode the presence of the jet exhaust flow on the wing surface, resulting from an on-the-wing nozzle installation, reduces the cruise performance by a number of ways including interaction and induced drag.

Engines, on the other hand, that are mounted a sufficient distance above the wing can minimize jet flow-wing interaction effects. Unpublished data indicate that location of the nozzle at about 0.1 chord height above the wing (fig. 1(c)) appears to yield an acceptable cruise performance. With such an OTW installation, an external deflector would be used to attach the engine flow to the wing-flap system for takeoff and landing. Such a system would probably require a variable deflector flap to minimize both the interaction noise and aerodynamic losses. Some additional weight penalties, however, can be expected to be associated with this system in order to provide for movement and storage of the deflector. For landing, the external deflector perhaps could also be used as a thrust reverser by proper articulation.

The present study, at model scale, is concerned with the effect of changes in the external deflector geometry on the aero-acoustic characteristics of a representative STOL-OTW configuration using an engine mounted above the wing. Principal geometry variables in the deflector include deflector size, deflector angle relative to the nozzle axis, and deflector type. Two types of external deflectors were used; a simple bent plate extending downstream from the nozzle (as in refs. 1, 2, 6, and 7) and a straight vane (airfoil-type). The latter represents, in a gross sense, a three-dimensional vane formed from a curved portion of the nacelle surface.

The conical nozzle had a diameter of 5.2 cm. Flap settings of 20° (takeoff) and 60° (landing) were used with a wing chords (flaps retracted) of 33 and 49.5 cm and a span of 61 cm (ref. 4). The nozzle was located at 0.1 chord (flaps retracted) downstream of the wing leading edge and 0.1 chord above the wing surface. The wing sizes are referred to herein as baseline (33 cm) and 3/2-baseline (49.5 cm). The aerodynamic data included lift and thrust force measurements. The acoustic data were obtained at directivity angles of 60°, 90°, and 120° measured from the inlet axis. The acoustic data are presented in terms of SPL spectra. All acoustic data were obtained at nominal cold-flow jet velocities of 200 and 259 m/sec.

APPARATUS AND PROCEDURE

Facilities

Lift-thrust facility. - Aerodynamic data consisting of lift and thrust components were obtained using the test stand (ref. 7) shown in figure 2. In this test stand pressurized air at about 289 K was applied to a 15.25-cm diameter plenum by twin diametrically opposed supply lines. Flexible couplings in each of the twin supply lines isolate the supply system from a force measuring system. The plenum is free to move axially and laterally through an overhead cable suspension system. The test nozzles, with and without wings, were attached to a flange at the downstream end of the

plenum. A load cell at the upstream end of the plenum is used to measure thrust. A second load cell is mounted near the nozzle to measure horizontal side loads. The wing-flap section was mounted in a vertical plane so that lift forces were measured by the side-mounted load cell (ref. 7).

Thrust and lift forces were obtained at nominal jet exhaust velocities of 200 and 266 m/sec. Airflow through the overhead supply line was measured with a calibrated orifice. The nozzle inlet total pressure was measured with a single probe near the plenum exit flange. Pressure data were recorded from suitable multitube manometers.

Acoustic facility. - The acoustic data were taken with the outdoor facility described in reference 7. In this facility, dry pressurized, ambient air was supplied to the nozzle/wing configurations through a control valve and valve-noise quieting system. This system consisted of a perforated plate, a four-chamber baffled muffler, and approximately 4.6 m of 10.16 cm diameter piping.

Acoustic data were taken using a horizontal semicircular array of microphones on a 3.05 m radius centered on the nozzle exhaust plane. The 1.27-cm omnidirectional condenser-type microphones used were in a plane level with the nozzle centerline. The microphone angles were at 60°, 90°, and 120° measured from the inlet. A mat of 15 cm thick acoustic foam was placed on the ground (asphalt) inside the microphone array to minimize ground reflections. The microphones were 1.52 m above ground level.

Microphone output signals were analyzed by a 1/3-octave-band spectrum analyzer. The analyzer determined sound pressure level (SPL) spectra referenced to 2×10^{-5} N/m^2. No ground reflection corrections were made to the noise data.

Acoustic measurements were taken over approximately the same range of jet exhaust velocities as those for the lift-thrust measurements; namely, 200 and 259 m/sec (jet Mach numbers of 0.6 and 0.8, respectively). All flow data for the acoustic tests were taken at cold-flow, ambient temperatures near 288 K.

Model Description

Nozzle and deflectors. -- The test nozzle was a conical nozzle with a
5. 2 cm diameter exit (fig. 3).

Two types of external flow deflectors were used in the study (fig. 3).
The first type consisted of a simple deflector vane (fig. 3(a)). The de-
flector vane was secured by two frames or "tracks" fastened to the
nozzle. The vane could be pivoted to various angles relative to the nozzle
centerline. The vane-type deflector was intended to provide the basis for
a practical design application. The second type consisted of a flat, hori-
zontal plate, parallel to the nozzle centerline, with a flap at the down-
stream end that was immersed in the jet exhaust flow (fig. 3(b)). These
deflectors were similar to those used in references 1, 2, 6, and 7 and
permit a direct comparison of the present data with that in these refer-
ences. Dimensions of all the deflectors are given in figure 3. All de-
flectors had a span of 7. 0 cm (1. 35 times the nozzle diameter). This
span represents a deflector width that can be stored within the confines
of an engine nacelle.

Wings. - The wings (shielding surfaces) are shown schematically in
figure 4 together with pertinent dimensions. The surfaces consisted of
metal plates secured to wooden ribs. The surfaces approximated the
upper surface contours of the airfoils with 20° and 60° deflected flaps
used in reference 4. All wings had a span of 61 cm. The nozzle was
mounted at the 0. 1 chord point of each wing and at 0. 1 chord above the
baseline wing. The 0. 1 chord point is based on the wing chord with
flaps retracted. The equivalent flaps-retracted chord sizes for these
wings are 33 and 49. 5 cm.

The wings will be referred to by the flap setting of 20° or 60°, and
their relative size is referred to as baseline (33 cm) and 3/2-baseline
(49. 5 cm).

AERODYNAMIC RESULTS

Weight Flow Considerations

In reference 1, it was established that if an external deflector is placed too close to the nozzle exhaust plane, particularly in conjunction with the proximity of a wing, a back pressure will be exerted on the flow resulting in a decrease in the nozzle weight flow. Consequently, in reference 1, the deflector was moved axially downstream until no weight flow reduction due to the deflector and wing was measured. The upstream end of the deflector (plate-type external deflector) in reference 1 was located about a nozzle radius from the nozzle exhaust plane. A similar location was selected for the deflectors in the present study. Weight flow measurements for all the nozzle/wing configurations herein showed no weight flow reductions due to back pressure effects on the flow system. For the nozzle alone and nozzle/wing configurations tested, the ratio of the measured to ideal weight flow was 0.98 and 0.99, respectively, for nominal jet Mach numbers of 0.6 and 0.8.

Lift and Thrust

The results of the lift and thrust measurements for the configurations tested are shown in figure 5. The lift and thrust forces are both ratioed to the nozzle alone thrust. The flow turning angle is referenced to the nozzle centerline axis. The magnitude of the radius represents the static flow turning efficiency; i.e. vectored thrust. The data shown in figure 5 are for jet Mach number of 0.8, flap settings of 20° and 60°, and both baseline and 3/2-baseline wings (similar results to those shown in this figure were obtained with a jet Mach number of 0.6; not shown herein). Also shown for comparison in figure 5 are lift-thrust data from references 3 and 7. In general the present data fall into the same aerodynamic performance range as that from references 3 and 7.

In terms of high lift and high thrust, the best aerodynamic performance with a 20° flap setting was obtained with the deflector penetrating into the jet flow to about the nozzle centerline. With a 60° flap setting a deeper

penetration into the jet flow by the deflector, of the order of 1/2 to 3/4 nozzle diameter, was required for the best aerodynamic performance. In addition, a somewhat larger deflector angle (5°-10° greater) was needed than those for the 20° flap setting. It should be noted that with a 20° deflector angle the flow, except with a 20° flap setting and the largest deflector (l = 7.9 cm), was either partially or completely detached from the wing surface, irrespective of wing size, flap setting and deflector size, resulting in high thrust but low lift.

As indicated by the square symbol data in figure 5, no significant differences in aerodynamic performance or trends were obtained between the vane-type and plate-type deflectors. Similar results were obtained for the other deflector sizes tested.

The following sections discuss in more detail the aerodynamic performance effects caused by changes in nozzle/wing geometry.

Effect of deflector size. - An increase in deflector length with a constant deflector angle resulted in a reduction in the measured vectored thrust (fig. 5). This effect was the result of an increase in spanwise flow caused by increasing the deflector size (length). The increase in spanwise flow generally decreased both the lift and thrust components of the vectored thrust. With a 20° flap setting, the flow turning angle (29°) was independent of deflector size as long as the flow was attached to the surface. With a 20° flap setting, the flow turning angle (29°) was independent of deflector size as long as the flow was attached to the surface. With a 60° flap setting and attached flow, the turning angle was somewhat more dependent on deflector size. Also from the data it is apparent that with reasonably well attached flow equal values of lift can be obtained from several deflector size and angle combinations; however, the thrust values may differ by as much as 50 percent for a 60° flap setting and nearly 10 percent for a 20° flap angle.

Effect of deflector angle. - Increased flow turning efficiency (vectored thrust) values were obtained for a constant deflector size with a decrease in deflector angle until significant flow separation became apparent. When partial or complete flow separation occurred, the flow turning efficiencies were generally of the order of 91 percent but the

lift was greatly reduced compared to that with attached flow. As mentioned previously, poor flow attachment was obtained with a 20° deflector angle. The optimum deflector angle appeared to be about 25° for a 20° flap setting and about 30° for a 60° flap setting.

Effect of wing size. - In general, with a 20° flap setting no significant differences in aerodynamic performance were observed for the two wings used in the tests. With a 60° flap setting, the flow turning angles were about 4° less with the 3/2-baseline wing than those with the baseline wing, while the flow turning efficiency (vectored thrust) was up to ~ percent less.

NOISE SOURCES

With a STOL-OTW configuration, the most prominent jet-associated noise sources, in the absence of core noise, are indicated in figure 6. These noise sources are: engine exhaust jet-mixing noise, deflector-flow generated interaction noise, fluctuating lift noise generated by flow over the wing surface, and trailing edge noise associated with the interaction between the edge and the jet flow. A typical OTW noise spectrum at $\theta = 90^O$ is shown schematically by the solid curve in figure 7. Also shown in the figure are curves for the nozzle with the external deflector (no wing) and for the nozzle alone. Addition of an external deflector to the nozzle causes a significant increase in the SPL over those for the nozzle alone, particularly in the mid and high frequency ranges of the spectrum. When the wing is added to the configuration the high frequency noise associated with both the nozzle alone and that for the nozzle-deflector configuration is attenuated (from a redirection of the noise by reflection from the source-side of the wing). The nozzle-deflector noise is also attenuated over a portion of the mid-frequency range. At low frequencies, jet interaction noise from the flow over the surface and the flap trailing edge increases the noise level over that of the nozzle alone.

ACOUSTIC RESULTS

The effect of the deflector geometry on the nozzle/wing system acoustics will be discussed primarily in terms of deflector type, deflector angle, and deflector length. The nozzle/wing noise spectra will be compared between the various geometries and that for the nozzle alone. The latter is used as an acoustic reference level to provide a criteria for ΔSPL values in the regions of jet/wing interaction noise and jet noise shielding. The measured acoustic data, in terms of spectra at directivity angles of 60°, 90°, and 120° are presented for a nominal jet Mach number of 0.8. Acoustic data and trends for a jet Mach number of 0.6 were similar to those obtained at a jet Mach number of 0.8 and are not included herein.

Effect of Deflector Type

Representative spectra for the vane- and plate-type deflectors with the baseline wings are shown in figure 8 for the 20^C flap setting and figure 9 for the 60° flap setting. The spectra are given for a directivity angle of 90° and for deflector angles of 25°, 30°, and 40°. The deflector length, l, for all the plate deflector data was 4.32 cm and 4.14 cm for the vane deflector data. It is apparent from these spectral plots that the spectra are essentially independent of the deflector types used. Similar results were obtained with both the shorter and longer deflector lengths, directivity angles of 60° and 120°, and with the 3/2-baseline wings.

On the basis of the preceding results, the subsequent acoustic data herein will be concerned only with the vane-type deflector because this deflector type appears most applicable, with suitable modifications for storage in an engine nacelle, to future OTW-STOL aircraft having the engines mounted above the wing.

Effect of Deflector Angle

Spectral plots are shown in figures 10 to 13 to illustrate the manner in which the acoustic spectra are affected by the deflector angle for con-

stant deflector length and flap setting. The data shown are for a 90° directivity angle. It should be noted that the data for a deflector length, l, of 1.95 cm is generally associated with detached flow, as evidenced by the small lift values given in figure 5.

Baseline wing. - In general, the low to mid frequency jet/wing interaction noise for powered lift tends to increase with increasing deflector angles (figs. 10 and 11). An exception to this trend occurred with the 40° deflector angle and a deflector length of 7.9 cm. For this configuration, the interaction noise SPL in the low and mid frequency ranges decrease relative to those for the 25° and 30° deflector angles.

With a 20° flap setting (fig. 10), the deflector angle had little effect on jet noise shielding at high frequencies except for the 40° deflector angle. This latter configuration had an additional noise source centered at about 8000 hertz. (Although this source appears tonal in nature, other data presented later indicates it is broadband or at least a broadband tone.) The SPL level and broadband width of this noise varied with deflector size and flap setting as is evident from figures 10 and 11 and later figures. Similar trends were also observed at the lower jet velocity of $M_j = 0.6$.

The noise source at 8000 hertz was believed to be generated by flow spillage around the sides of the deflector when too large a deflector angle is used. A brief check run was made using a deflector with twice the span of those used herein. The acoustic results from this check run showed that this noise source was increased rather than eliminated. Thus, the noise source centered at 8000 hertz has yet to be identified.

With a 60° flap setting (fig. 11), increasing the deflector angle tended to increase the SPL values; however, for powered lift ($\beta > 20°$) the effects generally were locally less than 5 dB except for the 40° deflector angle near 8000 hertz. Less jet noise shielding (about 3 dB at 20 000 hertz) was obtained with a 60° flap setting compared to that with a 20° flap setting.

3/2-baseline wing. - The acoustic trends caused by changes in the deflector angle noted with the baseline wing also occurred with the 3/2-baseline wing (figs. 12 and 13). The most notable difference in the data occurred in the shielding region at the high frequencies where no significant differences were observed with flap setting for the 3/2-baseline wing in contrast to the baseline wing where differences were observed.

Effect of Deflector Size

The effects of a change in deflector size (length) on the configuration spectra are shown in figures 14 to 17. The spectra are shown only for deflector angles of 25° and 30° which, as shown in figure 5, provide near optimum lift-thrust characteristics. The data shown in figures 14 to 17 are for a 90° directivity angle and a jet velocity of 259 m/sec (M_j = 0.8).

The spectra shown in figures 14 to 17 are for deflector lengths of 1.95, 4.14 and 7.90 cm. The latter two deflector lengths, according to figure 5, yield good powered lift characteristics for deflector angles of 25° and 30°. A deflector length of 1.95 cm generally showed low lift values which are attributed to detached flow from the wing surface, particularly in the case of a 60° flat setting. The latter aerodynamic data are not even included in figure 5. In the region of the jet/wing interaction noise for the cases of powered lift (attached flow), the SPL tended to increase somewhat (locally up to about 3 dB) with an increase in deflector length (square and diamond symbols in figs. 14 to 17). An exception occurred for some of the nozzle/wing configurations with the 30° deflector angle for which the SPL at low frequencies (<500 Hz) decreased by up to 5 dB with an increase in deflector length (figs. 15 to 17). Also shown in figures 14 to 17 are the spectra obtained with detached flow using the 1.95 cm deflector (circle symbols). As expected these SPL values are generally lower (locally as much as 11 dB for a 20° flap setting) than those with attached flow.

In the shielding region (high frequencies) the effect of deflector size on the SPL for powered lift varied with the particular configuration. In general, the variation of SPL was less than ±2 dB from the average for changes in the deflector length from 4.14 to 7.90 cm. The largest jet noise shielding benefits are obtained with the shortest deflector (1.95 cm); however, as noted previously, these benefits are only achieved when the flow is detached from the wing, not with powered lift.

Effect of Directivity Angle

Spectral data for the present nozzle/deflector/wing configurations also were obtained at directivity angles of 60° (forward quadrant) and 120° (rearward quadrant) in order to evaluate the effect of radiation angle on the interaction noise and jet noise shielding characteristics. The resulting spectra for powered lift are shown in figures 18 to 25.

Forward quadrant, $\theta = 60^O$. - For the most part, the interaction noise portion of the spectra for this directivity angle (figs. 18 to 21) show similar effects of deflector angle or size on the spectra as those noted for $\theta = 90^O$. The absolute SPL levels of the interaction noise in the low and mid-frequency range are less than those for a 90° directivity angle; however, the SPL differences between the interaction noise and the nozzle alone are similar.

In all cases, the data show considerably less jet noise shielding at high frequencies than that obtained at the 90° directivity angle. However, the amount of jet noise shielding obtained with a 25° deflector angle, a deflector length of 4.14 cm and the baseline wing is similar to that for comparable conical nozzle/wing configurations reported in references 1 and 2. The broadband noise centered at 8000 hertz also is much broader than that shown for the 90° directivity angle and is evident for deflector angles less than 40°.

Rearward quadrant, $\theta = 120^O$. - In general, the acoustic data trends with the various configuration geometries for a directivity angle of 120° were similar to those for the 90° directivity angle as shown in figures 22 to 25. The data obtained with a 20° deflector angle and a deflector width of 4.14 cm showed abnormally high SPL values in the high frequency range using the baseline wing for both the 20° and 60° flap angles. No reasons are advanced at this time to account for these abnormalities.

Effect of Wing Size

The general effect of wing size on the acoustic characteristics is shown in figure 26. The spectra shown are for a deflector angle of 25°, a deflector length of 4.14 cm and both the 20° and 60° flap settings.

The increase in wing size from baseline to 3/2-baseline caused nearly all of the SPL values to decrease. An exception to this trend occurred at frequencies less than 300 hertz. Also, except for local variations in the SPL values, the acoustic data trends with increasing wing size are similar for both the 20° and 60° flap settings. As expected, significantly larger jet noise shielding benefits were obtained with the 3/2-baseline wing when compared to those obtained with the baseline wing. Shielding of the jet noise is evident for frequencies greater than about 1250 hertz with the 3/2-baseline wing whereas significant shielding is evident only for frequencies greater than 8000 hertz wit' 'he baseline wing. These overall trends also vere observed for the o'' ar configurations used, although the changes in the specific SPL magnitudes for given frequencies varied with each configuration.

Comparison of OTW Above-Wing Spectra with On-Wing Spectra

A representative spectrum from the present study is compared in figure 27 with that from the 5:1 aspect ratio slot used in the nozzle work reported in reference 4. In the latter study the nozzle was mounted directly on the wing at the 21 percent chord station of the same baseline wing used herein. Both sets of data shown are for a 20° flap setting and a nominal jet Mach number of 0.8. The data are for a deflector angle of 30° and a deflector length of 4.14 cm for the present data, while the slot nozzle had a nozzle roof angle of 30° and a 30° nozzle sidewall cutback angle. Both configurations had about the same lift and thrust characteristics. It is apparent from the data that the overall spectra are quite similar. The present configuration has somewhat lower SPL values in the mid frequencies than those with the slot nozzle; however, this may be a particular configuration related idiosyncracy.

CONCLUDING REMARKS

The data reported in the present work and that with on-the-wing slot nozzle OTW configurations (refs. 3 and 4) indicate that the optimum

aerodynamic performance is associated with the maximum noise levels for a configuration. A tradeoff in terms of reduced aerodynamic performance for a given nozzle/wing configuration does not significantly alter the noise levels.

The primary criteria for the selection of an OTW nozzle/wing configuration may well be the cruise performance for which a three dimensionally curved external deflector (storable as part of the nacelle) with the engine mounted above the wing may provide an optimum design from both aerodynamic and acoustic tradeoff considerations. The external deflector storage for cruise can also perhaps be facilitated by use of an inverted "D-nozzle" for which the flat portion of the "D" would provide storage space for the deflector. An OTW configuration with such a nozzle and using an external deflector should provide essentially the same aerodynamic performance and acoustic characteristics as that using a conical nozzle with an external deflector.

NOMENCLATURE

(All data are in SI units)

A, B, C, Y	deflector dimensions (figs. 3 and 4)
c	chord
L	measured lift
L_f	wing length upstream of nozzle exhaust plane
L_p	projected shielding surface length
L_s	shielding surface length
l	effective deflector length
M_j	jet Mach number
SPL	sound pressure level, dB re 2×10^{-5} N/m^2
T	measured configuration thrust
T_j	jet thrust (nozzle alone)

U_j jet exhaust velocity

α flap setting

β deflector angle

θ directivity angle

η turning efficiency

REFERENCES

1. Reshotko, M., Olsen, W. A., and Dorsch, R. G., "Preliminary Noise Tests of the Engine-Over-the-Wing Concept. I. 30°-60° Flap Position," TM X-68032, Mar. 1972, NASA.

2. Reshotko, M., Olsen, W. A., and Dorsch, R. G., "Preliminary Noise Tests of the Engine-Over-the-Wing Concept. II. 10°-20° Flap Position," TM X-68104, June 1972, NASA.

3. von Glahn, U. and Groesbeck, D., "Nozzle and Wing Geometry Effects on OTW Aerodynamic Characteristics," AIAA Paper 76-622, July 1976, Palo Alto, Calif.

4. von Glahn, U. and Groesbeck, D., "Geometry Effects on STOL Engine-Over-the-Wing Acoustics with 5:1 Slot Nozzle," TM X-71820, 1975, NASA.

5. von Glahn, U. and Groesbeck, D., "OTW Noise Correlation for Variations in Nozzle/Wing Geometry with 5:1 Slot Nozzles," AIAA Paper 76-521, July 1976, Palo Alto, Calif.

6. Reshotko, M., Goodykoontz, J. H., and Dorsch, R. G., "Engine-Over-the-Wing Noise Research," TM X-68246, 1973, NASA.

7. Reshotko, M., and Friedman, "Acoustic Investigation of the Engine-Over-the-Wing Concept Using a D-Shaped Nozzle," AIAA Paper 73-1030, Oct. 1973, Seattle, Wash.
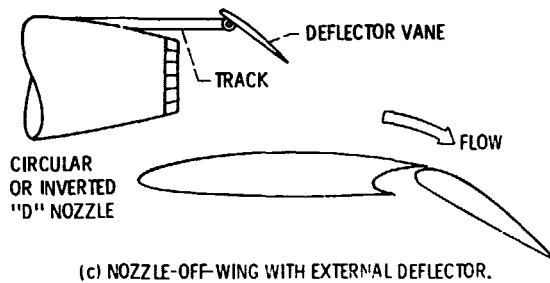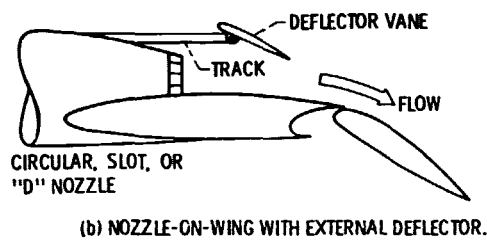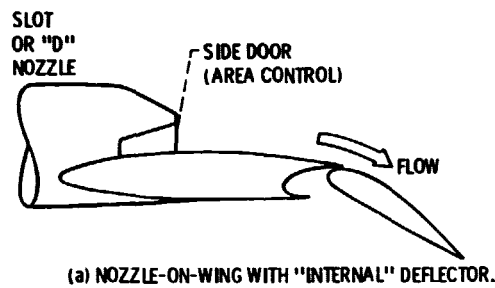
Figure 1. - Conceptual OTW nozzle/wing configurations.

SLOT
OR "D"
NOZZLE

SIDE DOOR
(AREA CONTROL)

FLOW

(a) NOZZLE-ON-WING WITH "INTERNAL" DEFLECTOR.

DEFLECTOR VANE

TRACK

FLOW

CIRCULAR, SLOT, OR
"D" NOZZLE

(b) NOZZLE-ON-WING WITH EXTERNAL DEFLECTOR.

DEFLECTOR VANE

TRACK

FLOW

CIRCULAR
OR INVERTED
"D" NOZZLE

(c) NOZZLE-OFF-WING WITH EXTERNAL DEFLECTOR.
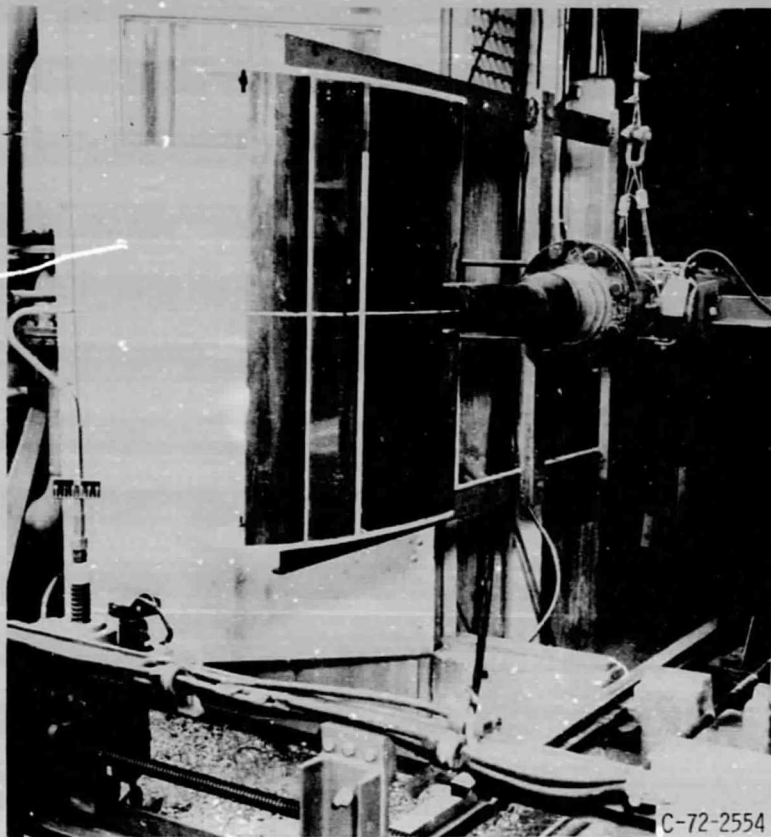
Figure 2. – OTW configuration in the lift-thrust facility (ref. 7).

β	ℓ	A	B
20°	2.16	4.65	0.68
	4.32	6.73	1.41
	8.13	10.29	2.76
25°	4.32	6.50	1.87
	8.13	9.98	3.52
30°	2.16	4.50	1.04
	4.32	6.35	2.13
	8.13	9.73	4.01
40°	2.16	4.30	1.34
	4.32	5.97	2.76
	8.13	8.94	5.22

(b) PLATE-TYPE DEFLECTORS.

Figure 3. - Concluded.

ℓ	A	B	C	β
1.95	2.41	1.04	3.86	20°
	2.24	1.21	3.63	25°
	2.13	1.32	3.51	30°
	2.03	1.42	3.25	40°
4.14	2.51	3.18	3.91	20°
	2.29	3.40	3.66	25°
	2.18	3.51	3.51	30°
	2.06	3.63	3.25	40°
7.90	2.54	6.91	4.01	20°
	2.31	7.14	3.66	25°
	2.11	7.34	3.40	30°
	2.03	7.42	3.18	40°

(a) VANE-TYPE DEFLECTORS.

Figure 3. - Schematic sketches of nozzle and flow deflectors. (All dimensions in centimeters.)

E-8823
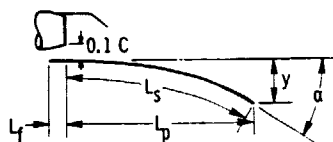
WING DIMENSIONS

FLAP ANGLE, α, DEG	CONFIGURATION	y, CM	L_f, CM	L_p, CM	L_s, CM
20	BASELINE	6.6	3.3	37.4	39.0
	3/2-BASELINE	10.2	5.0	56.0	58.4
60	BASELINE	14.3	3.3	34.1	42.3
	3/2-BASELINE	21.5	5.0	50.9	62.8

Figure 4. - Wing dimensions.

Figure 5. - Static turning effectiveness for various nozzle/wing configurations; M_j, 0.8.
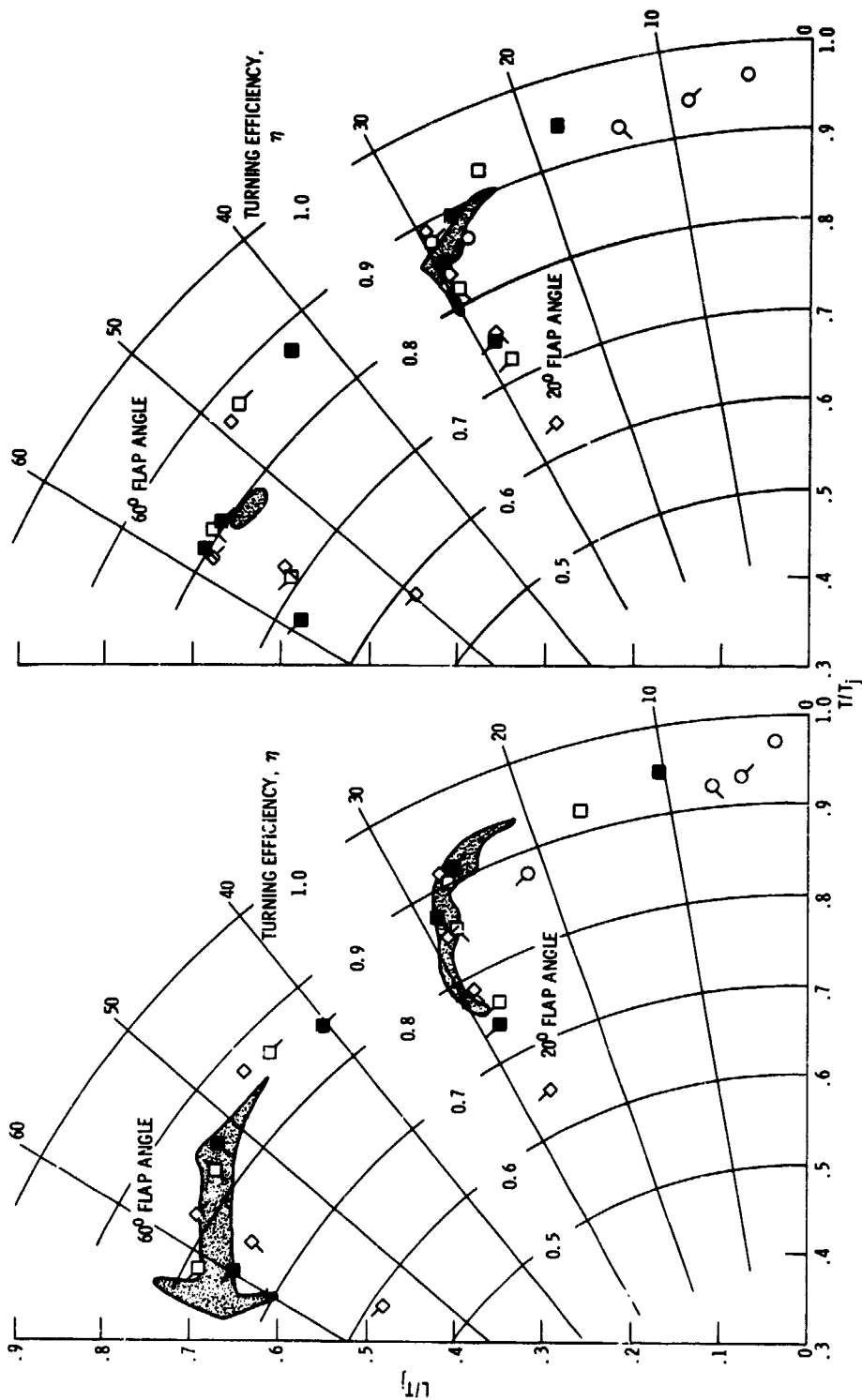
(a) BASELINE WING.

(b) 3/2-BASELINE WING.
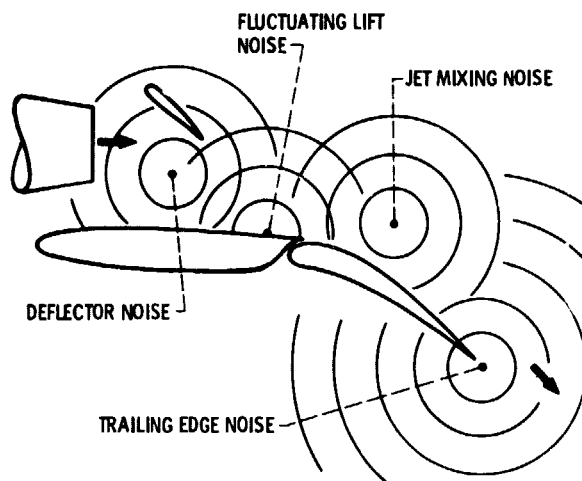
Figure 6. - Noise sources for OTW configuration with external deflector.
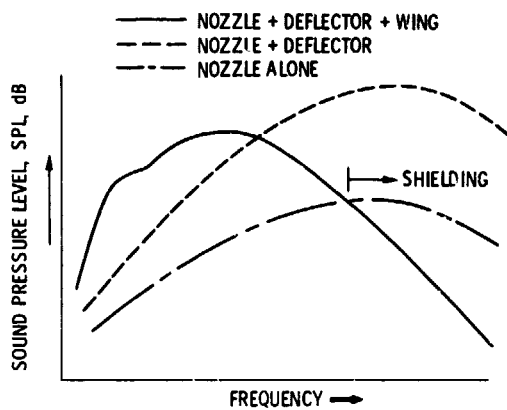
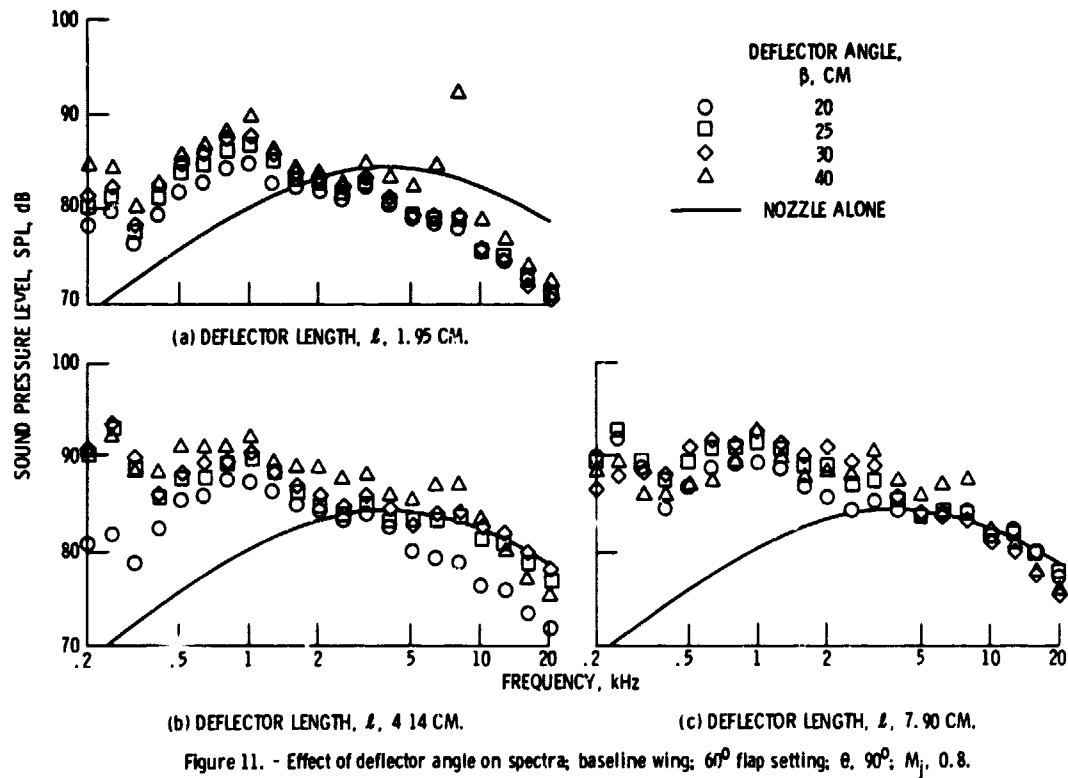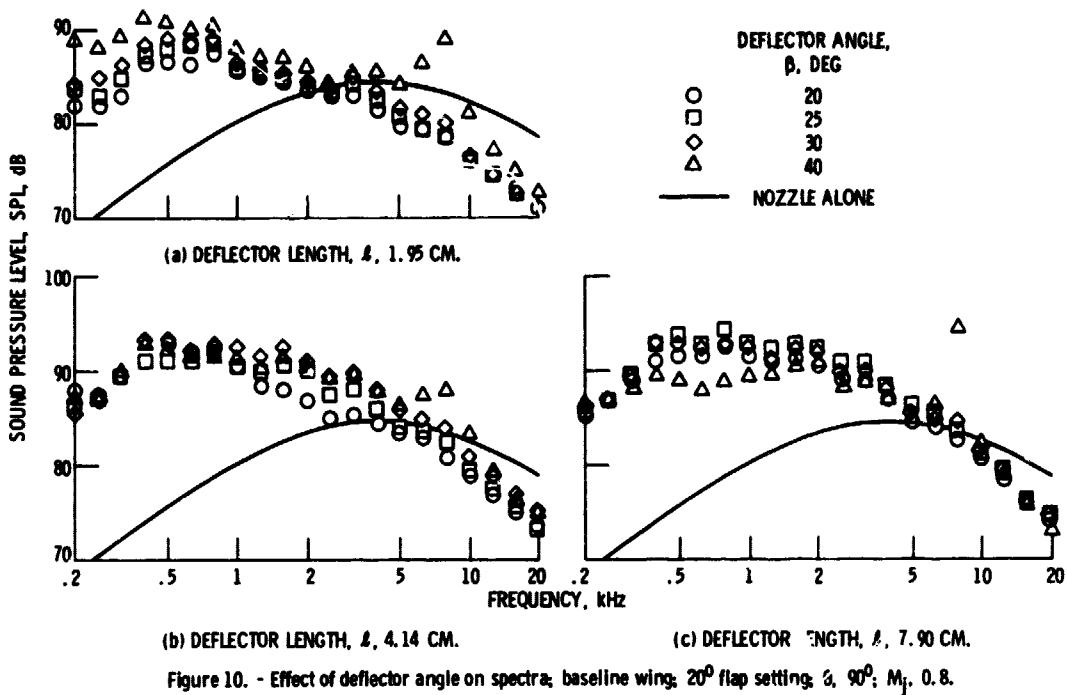Figure 7. - Representative spectra for OTW configuration with an external deflector; θ = 90°.
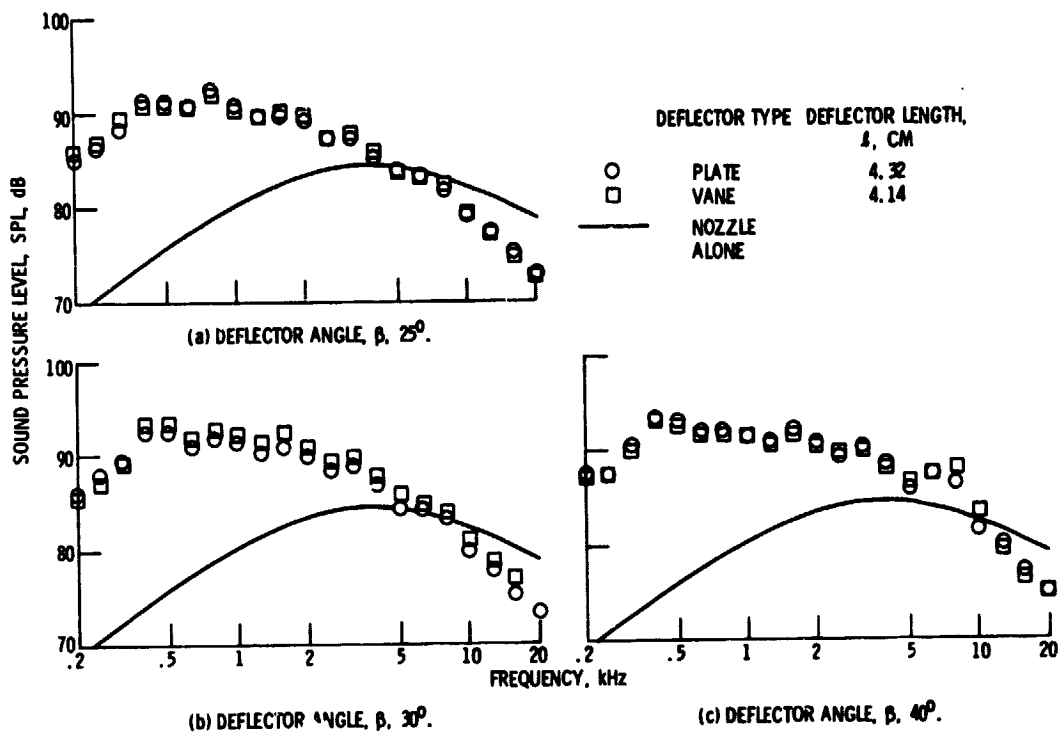
Figure 8. - Comparisons of representative spectra for vane- and plate-type external deflectors using baseline wing with 20° flap setting; M_j, 0.8; θ, 90°.
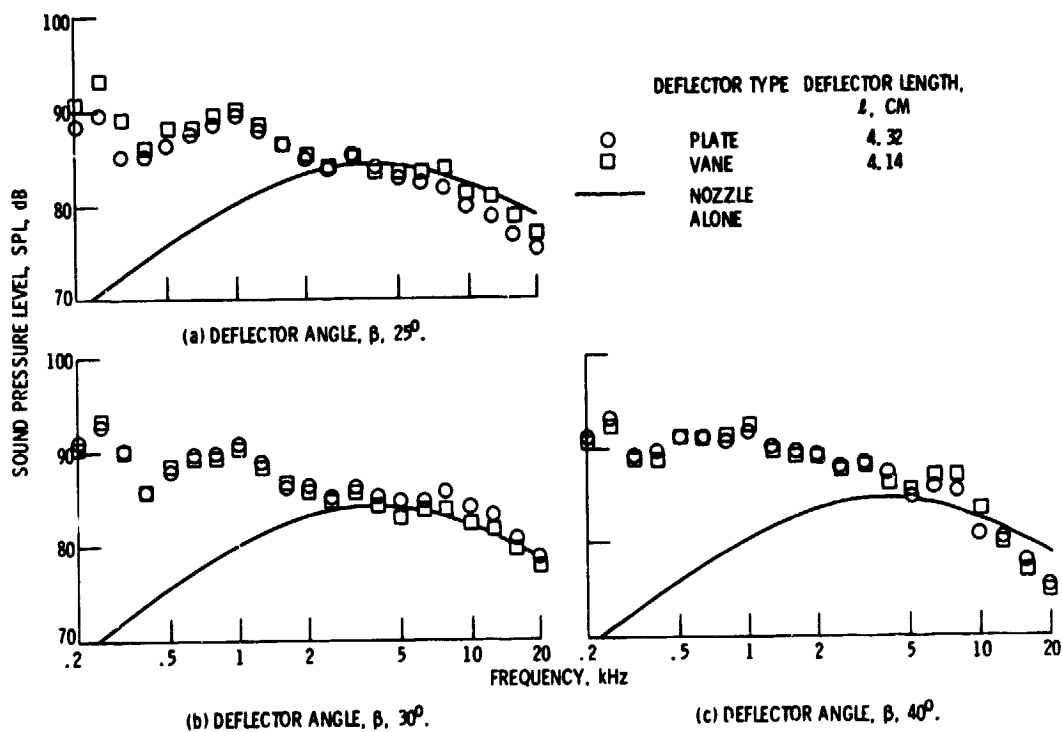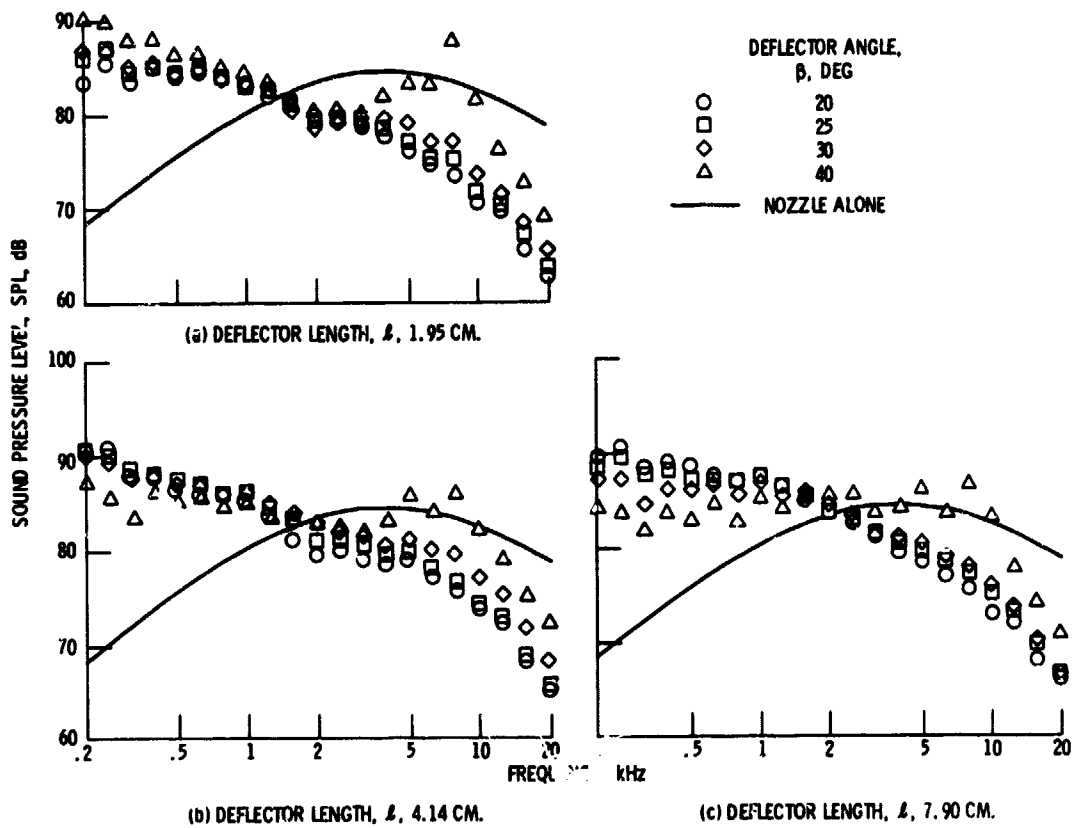

Figure 9. - Comparisons of representative spectra for vane- and plate-type external deflectors using baseline wing with 60° flap setting; M_j, 0.8; θ, 90°.

Figure 10. - Effect of deflector angle on spectra; baseline wing; 20° flap setting; θ, 90°; M_j, 0.8.
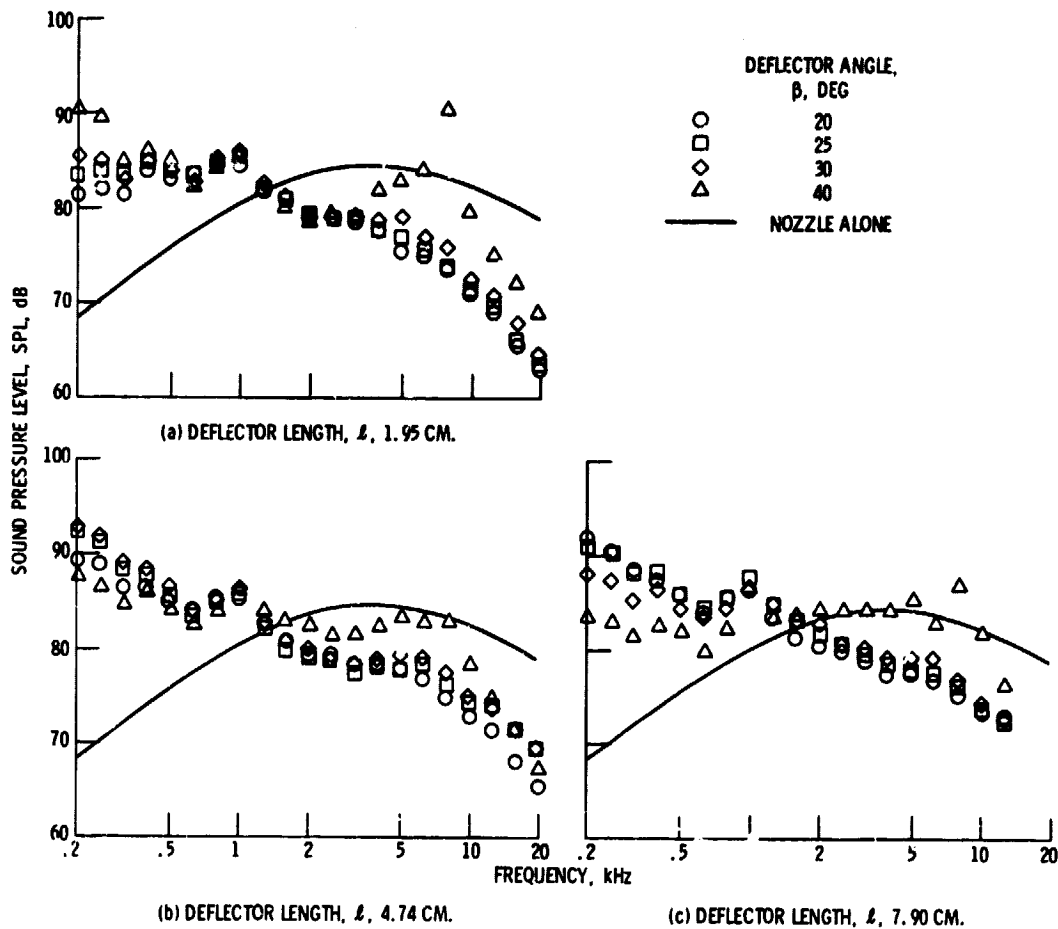
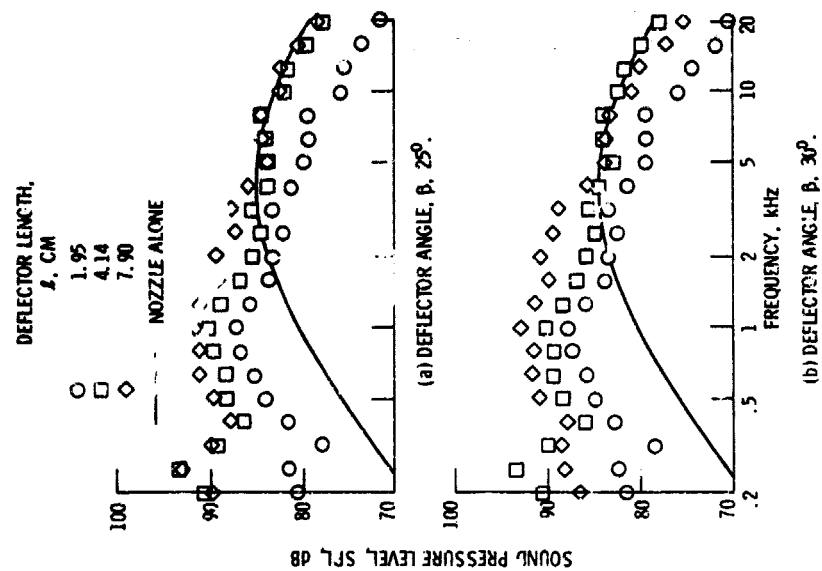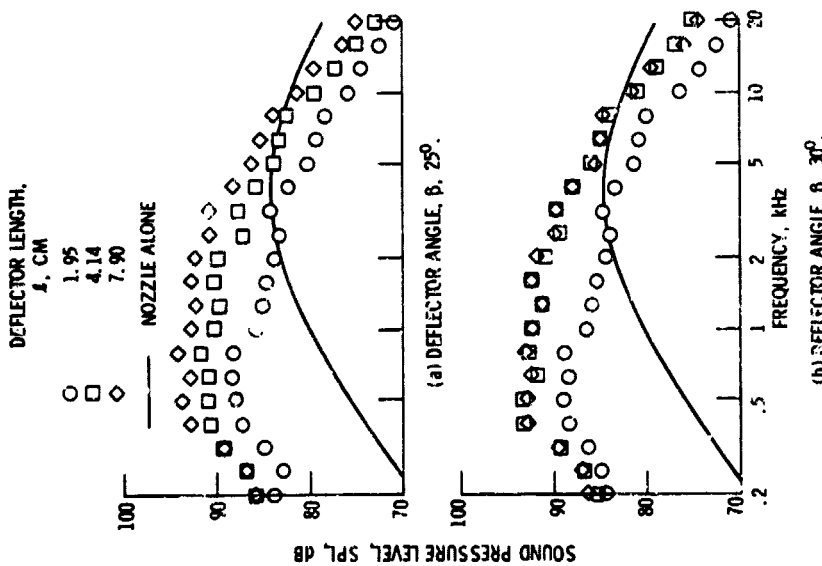Figure 11. - Effect of deflector angle on spectra; baseline wing; 60° flap setting; θ, 90°; M_j, 0.8.

Figure 12. - Effect of deflector angle on spectra; 3/2-baseline wing; 20° fl , setting; θ, 90°; Mⱼ, 0.8.

Figure 13. – Effect of deflector angle on spectra; 3/2-baseline wing; 60° flap setting; θ, 90°; M_j, 0.8.

DEFLECTOR LENGTH,
ℓ, CM

○   1.95
□   4.14
◇   7.90

——   NOZZLE ALONE

(a) DEFLECTOR ANGLE, β, 25°.

(b) DEFLECTOR ANGLE, β, 30°.

SOUND PRESSURE LEVEL, SPL, dB

FREQUENCY, kHz

Figure 15. – Effect of deflector length on spectra; baseline wing; 60° flap setting; θ, 90°; M_j, 0.8.

DEFLECTOR LENGTH,
ℓ, CM

○   1.95
□   4.14
◇   7.90

——   NOZZLE ALONE

(a) DEFLECTOR ANGLE, β, 25°.

(b) DEFLECTOR ANGLE, β, 30°.

SOUND PRESSURE LEVEL, SPL, dB

FREQUENCY, kHz

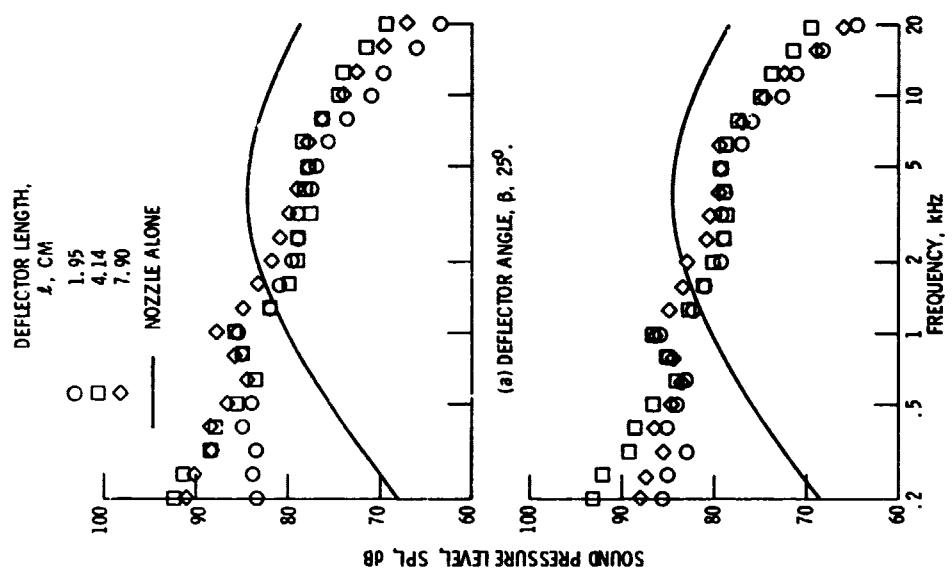Figure 14. – Effect of deflector length on spectra; baseline wing; 20° flap setting; θ, 90°; M_j, 0.8.

Figure 17. – Effect of deflector length on spectra; 3/2-baseline wing; 60° flap setting; θ, 90°; M$_j$, 0.8.

Figure 16. – Effect of deflector length on spectra; 3/2-baseline wing; 20° flap setting; θ, 90°; M$_j$, 0.8.
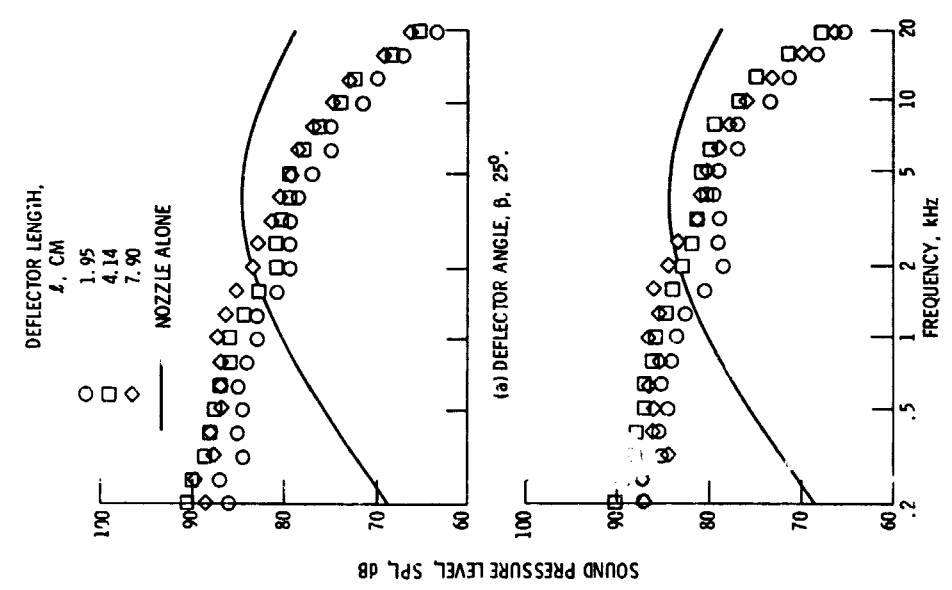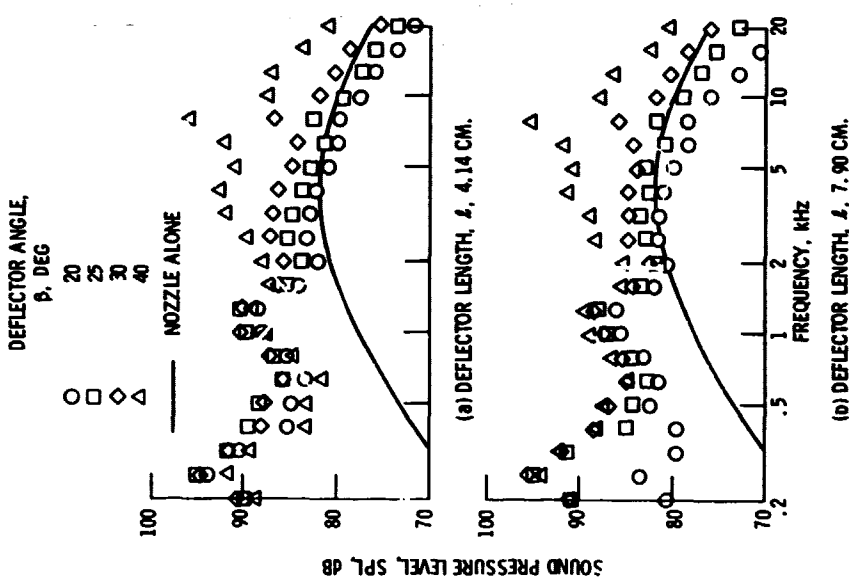
DEFLECTOR ANGLE,
β, DEG
20
25
30
40

NOZZLE ALONE

(a) DEFLECTOR LENGTH, ℓ, 4.14 CM.

(b) DEFLECTOR LENGTH, ℓ, 7.90 CM.

FREQUENCY, kHz

SOUND PRESSURE LEVEL, SPL, dB
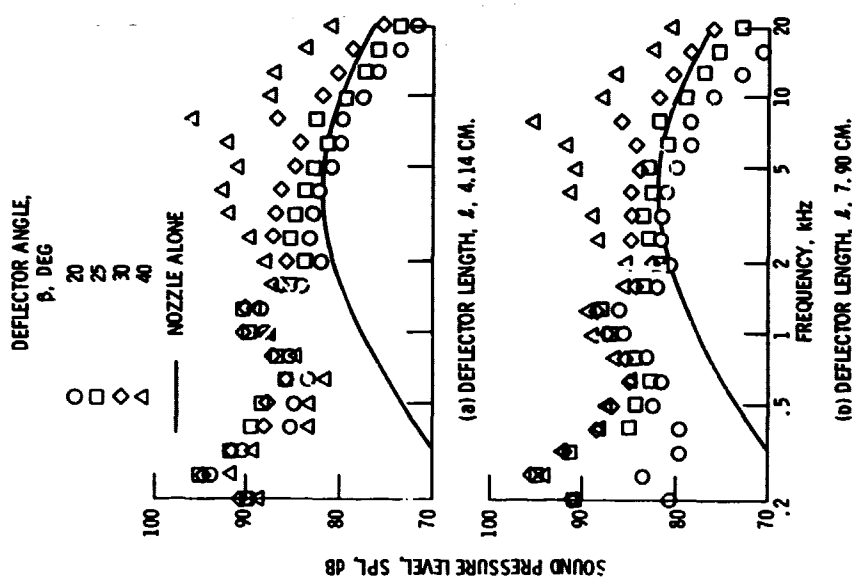
Figure 19. – Effect of deflector angle on spectra in for ard quadrant using baseline wing; θ, 60°; 60° flap setting; M_j, 0.8.

DEFLECTOR ANGLE,
β, DEG
20
25
30
40

NOZZLE ALONE

(a) DEFLECTOR LENGTH, ℓ, 4.14 CM.

(b) DEFLECTOR LENGTH, ℓ, 7.90 CM.

FREQUENCY, kHz

SOUND PRESSURE LEVEL, SPL, dB
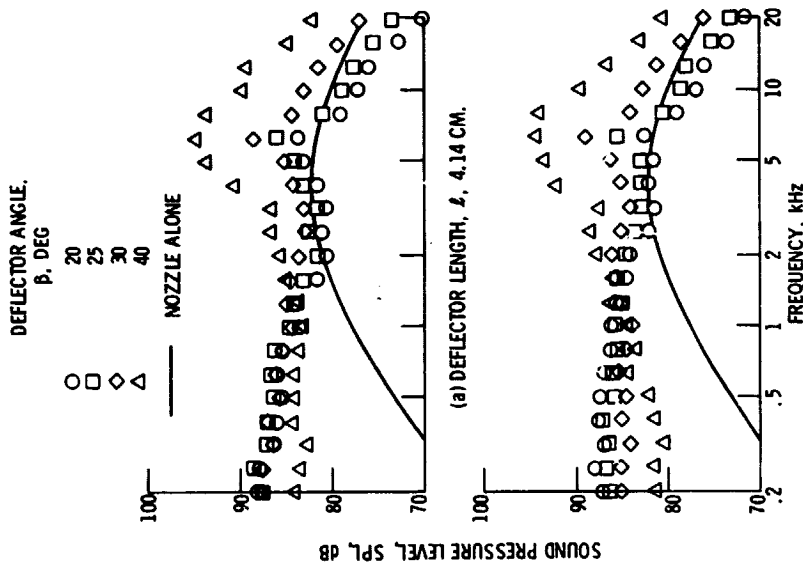
Figure 18. – Effect of deflector angle on spectra in forward quadrant using baseline wing; θ, 60°; 20° flap setting; M_j, 0.8.

DEFLECTOR ANGLE,
β, DEG
20
25
30
40

NOZZLE ALONE

SOUND PRESSURE LEVEL, SPL, dB

(a) DEFLECTOR LENGTH, ℓ, 4.14 CM.

FREQUENCY, kHz

(b) DEFLECTOR LENGTH, ℓ, 7.90 CM.
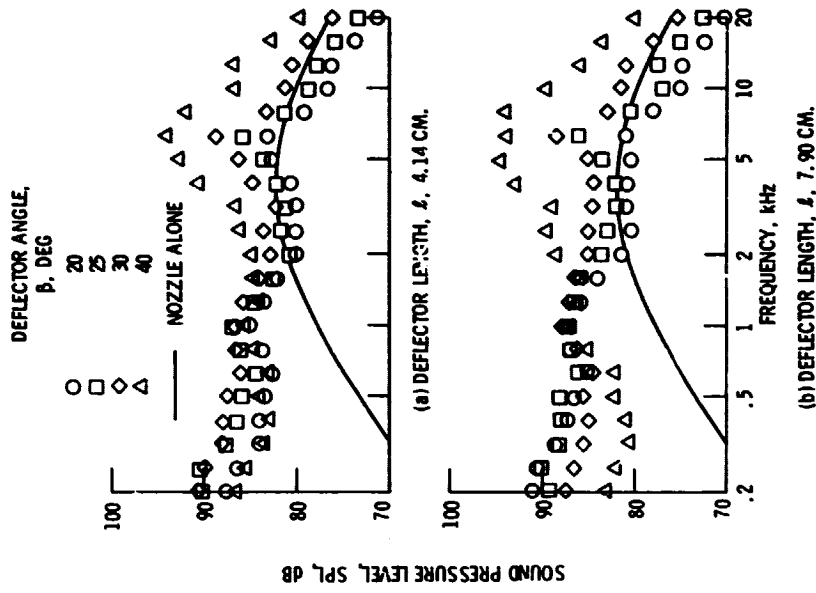
Figure 21. – Effect of deflector angle on spectra in forward quadrant using 3/2-baseline wing: θ, 60°; 60° flap setting; M_j, 0.8.

DEFLECTOR ANGLE,
β, DEG
20
25
30
40

NOZZLE ALONE

SOUND PRESSURE LEVEL, SPL, dB

(a) DEFLECTOR LENGTH, ℓ, 4.14 CM.

FREQUENCY, kHz

(b) DEFLECTOR LENGTH, ℓ, 7.90 CM.

Figure 20. – Effect of deflector angle on spectra in forward quadrant using 3/2-baseline wing: θ, 60°; 20° flap setting; M_j, 0.8.

E-8823

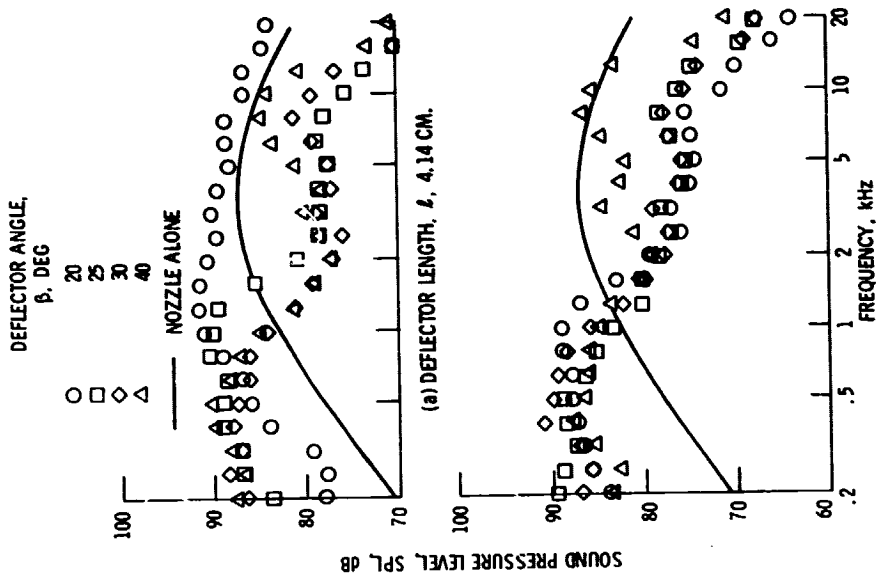DEFLECTOR ANGLE,
β, DEG
○ 20
□ 25
◇ 30
△ 40

─── NOZZLE ALONE

(a) DEFLECTOR LENGTH, ℓ, 4.14 CM.

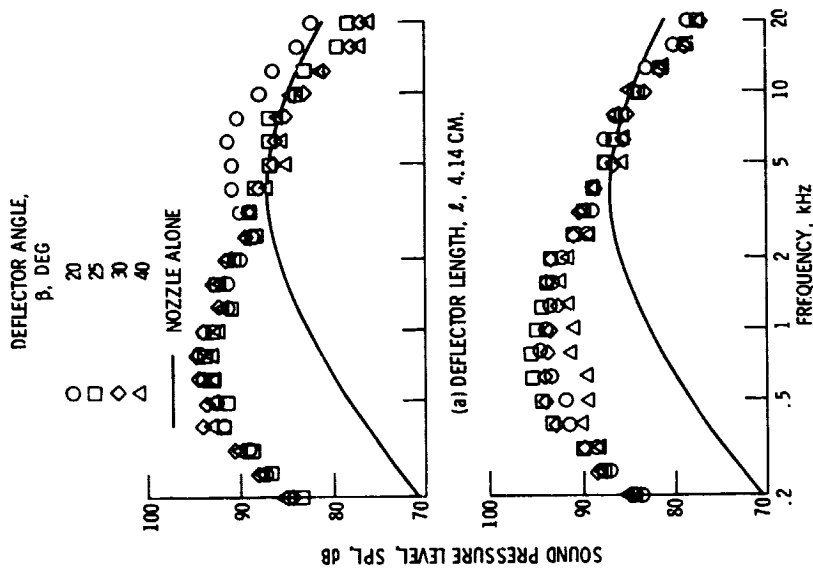(b) DEFLECTOR LENGTH, ℓ, 7.90 CM.

SOUND PRESSURE LEVEL, SPL, dB

FREQUENCY, kHz

Figure 23. - Effect of deflector angle on spectra in rear-ward quadrant using baseline wing; θ, 120°; 60° flap setting; M_j, 0.8.

DEFLECTOR ANGLE,
β, DEG
○ 20
□ 25
◇ 30
△ 40

─── NOZZLE ALONE

(a) DEFLECTOR LENGTH, ℓ, 4.14 CM.

(b) DEFLECTOR LENGTH, ℓ, 7.90 CM.

SOUND PRESSURE LEVEL, SPL, dB

FREQUENCY, kHz

Figure 22. - Effect of deflector angle on spectra in rear-ward quadrant using baseline wing; θ, 120°; 20° flap setting; M_j, 0.8.
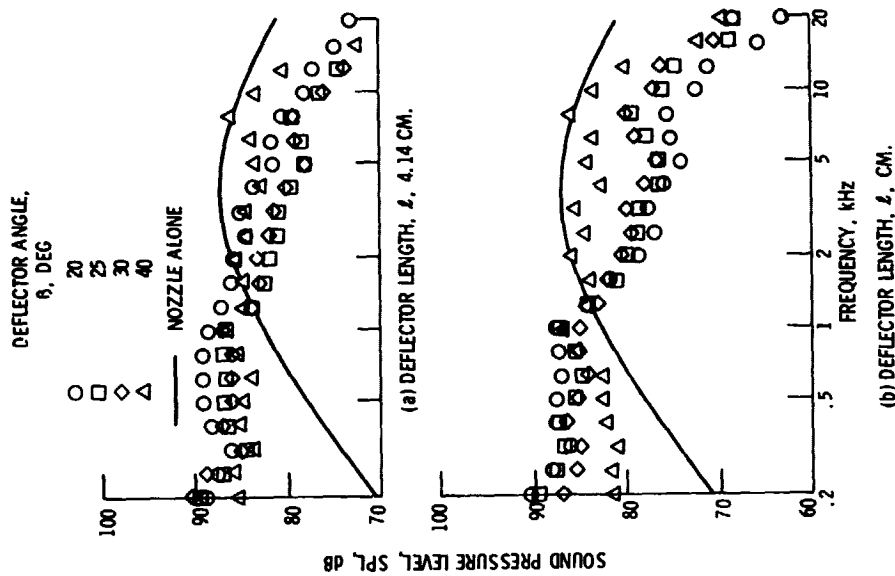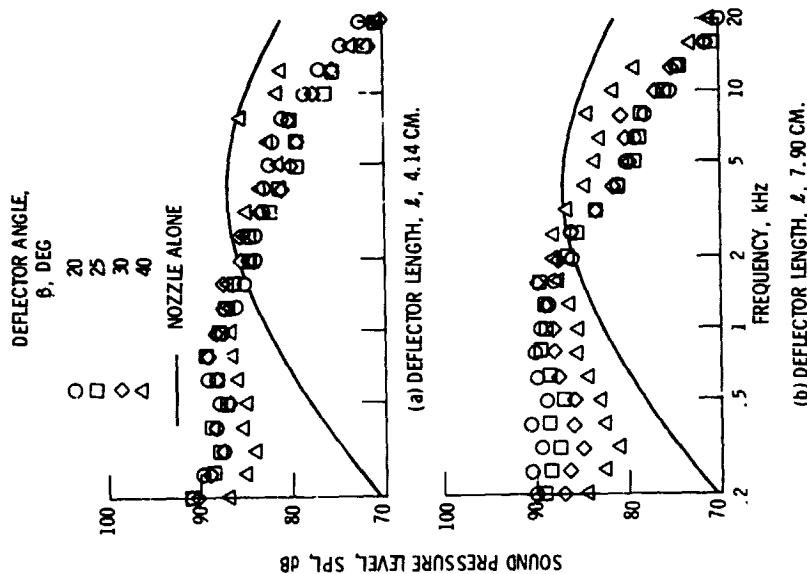
Figure 24. – Effect of deflector angle on spectra in rear-ward quadrant using 3/2-baseline wing; θ, 120°; 20° flap setting; M_j, 0.8.
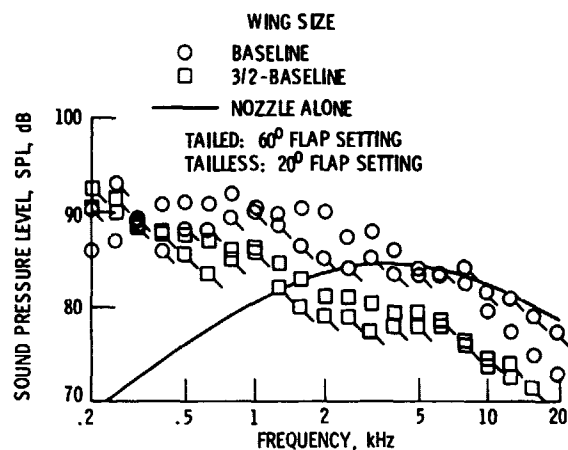
Figure 25. – Effect of deflector angle on spectra in rear-ward quadrant using 3/2-baseline wing; θ, 120°; 60° flap setting; M_j, 0.8.

WING SIZE

○ BASELINE
□ 3/2-BASELINE
── NOZZLE ALONE

TAILED: 60° FLAP SETTING
TAILLESS: 20° FLAP SETTING

Figure 26. - Representative effect of wing size on noise spectra. Deflector angle, β, 25°; deflector length, ℓ, 4.14 cm; θ, 90°; M_j, 0.8.

○ CONICAL NOZZLE, DEFLECTOR, AND
    WING (PRESENT WORK)
□ 30/30 SLOT NOZZLE/WING
── CONICAL NOZZLE ALONE
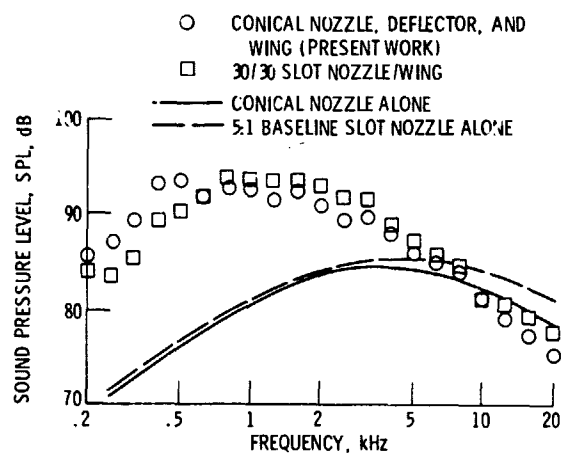── 5:1 BASELINE SLOT NOZZLE ALONE

Figure 27. - Spectral comparison of 5:1 slot nozzle/wing (ref. 3) with comparable external deflector OTW configuration. Baseline wing; 20° flap setting; β, 30°; ℓ, 4.14 cm; θ, 90°; M_j, 0.8.